Supplementary Material

Text S1 Catalyst characterization and the evaluation of activity for CO oxidation

Catalyst characterization

The X-ray diffraction (XRD) patterns were obtained on the Bruker X-ray diffractometer (D8-Advance, Bruker, Germany) equipped with Cu-Kα X-ray source. SEM images were recorded on a Merlin SEM microscope (Carl Zeiss, Germany). TEM images were acquired on a JEOL-2011 instrument (JEOL, Japan). X-ray photoelectron spectroscopy (XPS) were measured on an ESCALAB 250Xi X-ray photoelectron spectrometer (Thermo Fisher, USA) and the binding energy was calibrated with the C 1s peak at 284.8 eV. Raman spectra were obtained on a Britain inVia spectrometer. The specific surface area and pore size distribution were determined on a Micromeriticis ASAP 2020 analyzer (USA), using the nitrogen adsorption data at 77K. The element contents of catalysts were determined by inductively coupled plasma-optical emission spectroscopy (ICP-OES, Thermo IRIS Intrepid II XSP, USA).

H_2 temperature programmed reduction (H_2-TPR) and O_2 temperature programmed desorption (O_2-TPD) were performed on an AutoChem II 2920 instrument (Micromeritics, USA) equipped with a thermal conductivity detector (TCD). Prior to testing, 50 mg samples (40–60 meshes) were pretreated at 105℃ for 30 min in the helium flow. For the H_2-TPR measurement, the sample was programmed to rise to 800℃ at a ramp rate of 5℃/min in 5% H_2/Ar atmosphere. For the O_2-TPD analysis, the sample was purged with 5% O_2/He for 30 min and then by helium for another 30 min. Subsequently, it was heated from 40℃ to 800℃ at a ramp rate of 5℃/min in the helium flow.

In situ diffuse reflectance infrared Fourier transform spectra (DRIFTS) was performed on a Nicolet 6700 FTIR (Thermo Fisher, USA) to detect the surface change of sample during CO adsorption and oxidation. Before the testing, the sample was pretreated at 105℃ in N_2 flow for 2 h and cooled to 35℃.

Evaluation of activity for CO oxidation

The catalytic performance for CO oxidation was evaluated in a quartz tube reactor with the inner diameter of 6 mm. Unless otherwise noted, 100 mg catalyst powder with the size of 40–60 mesh was used. The reactor was placed in a pipe furnace, which can programed temperature and maintained at each set temperature for 30 min. The total flow rate of was 250 mL/min with the corresponding weight hourly space velocity (WHSV) of 150 L/g·h. The inlet CO concentration was 250 ppm balanced with synthesized air, and the water content was adjusted by adjusting the flow rate through the water bath and was measured by a hygrometer (testo 635-2) with an accuracy of 0.1%. The concentrations of CO and CO_2 was monitored online by GC-2014 (Shimadzu, Japan) equipped with a flame ionization detector and a methanizer. The CO conversion ratio was calculated using the following equation (Eq. (S1)):

$$\text{CO conversion} = \frac{C_{inlet} - C_{outlet}}{C_{inlet}} \times 100\% \quad , \qquad \text{(S1)}$$

where C_{inlet} and C_{outlet} are the inlet and outlet CO concentration, respectively.

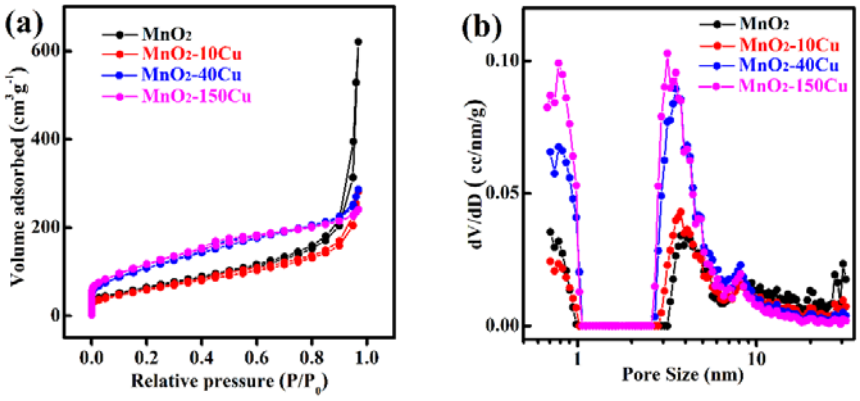

Fig. S1 (a) Nitrogen adsorption-desorption curves and (b) pore distributions of catalysts.

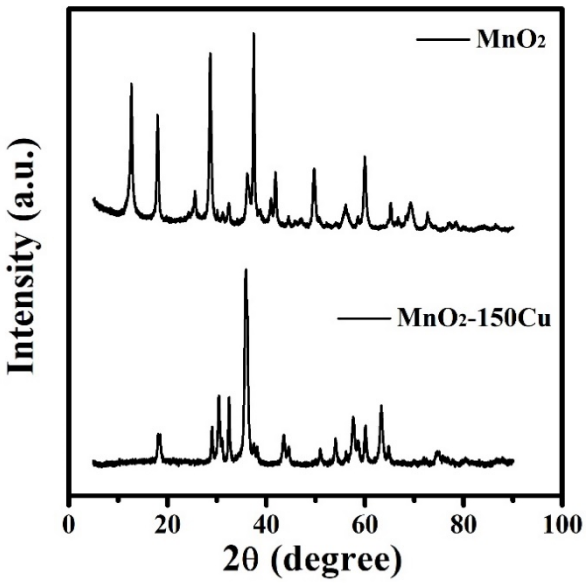

Fig. S2 The XRD patterns of MnO_2 and MnO_2-150Cu after treated in O_2-TPD until 500℃.

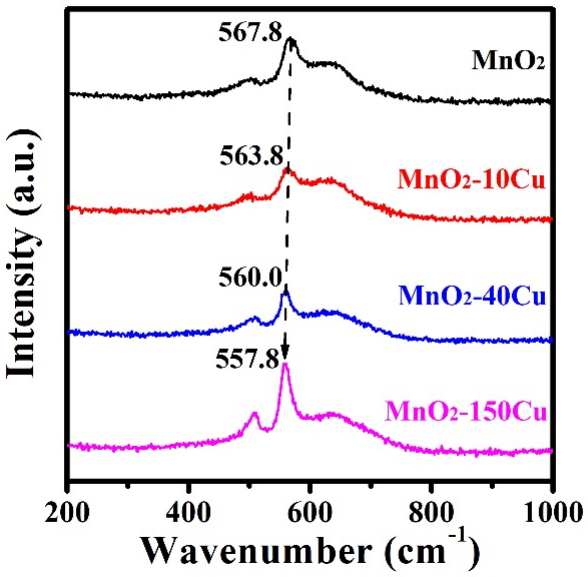

Fig. S3 Raman spectra of different samples.

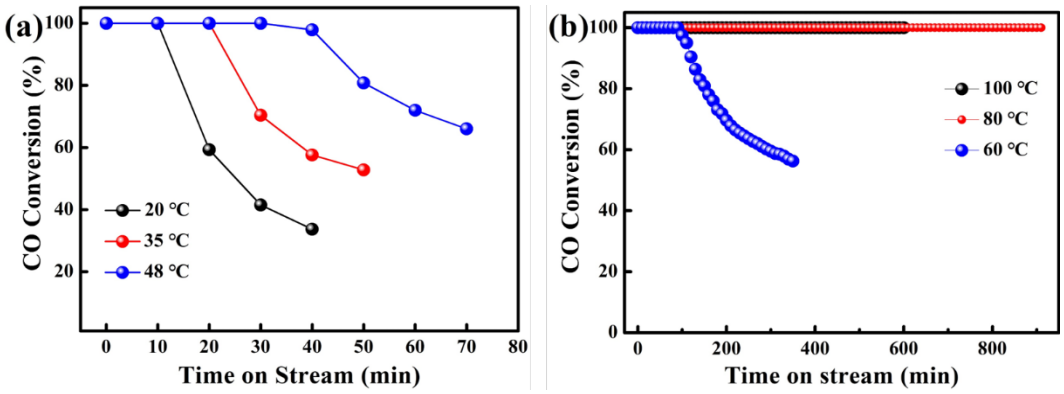

Fig. S4 The performance of MnO_2-150Cu for 1% CO conversion under dry air condition at different temperatures under the WHSV of 35 L/g·h. (a) 20℃, 35℃ and 48℃; (b) 60℃, 80℃ and 100℃.

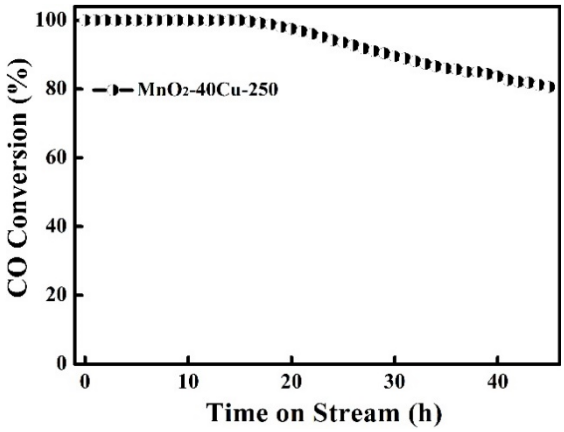

Fig. S5 The performance of MnO_2-40Cu after it was heated at 250℃ for 4 h (Test conditions: CO inlet concentration 250 ppm, temperature 20℃, WHSV 150 L/g·h, dry air).

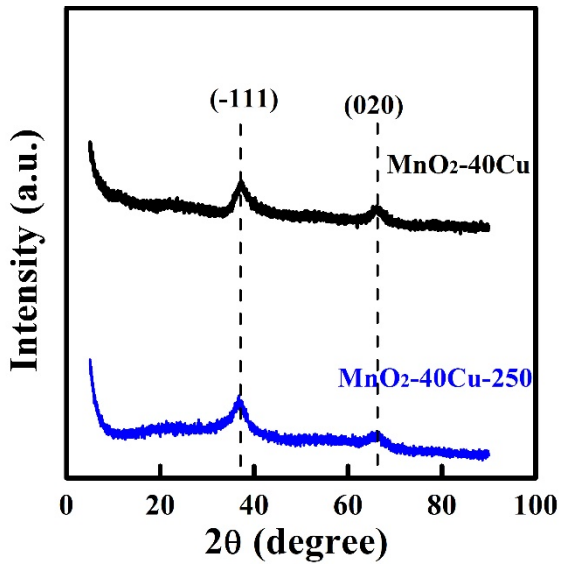

Fig. S6 XRD patterns of MnO_2-40Cu before and after heated at 250℃ for 4 h.

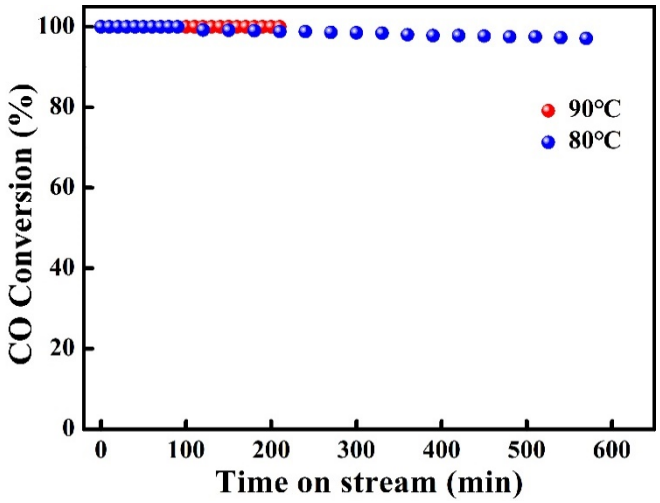

Fig. S7 The performance of MnO_2-150Cu for 1% CO conversion under humid air condition (3%) at 80℃ and 90℃ under the WHSV of 40 L/g·h.

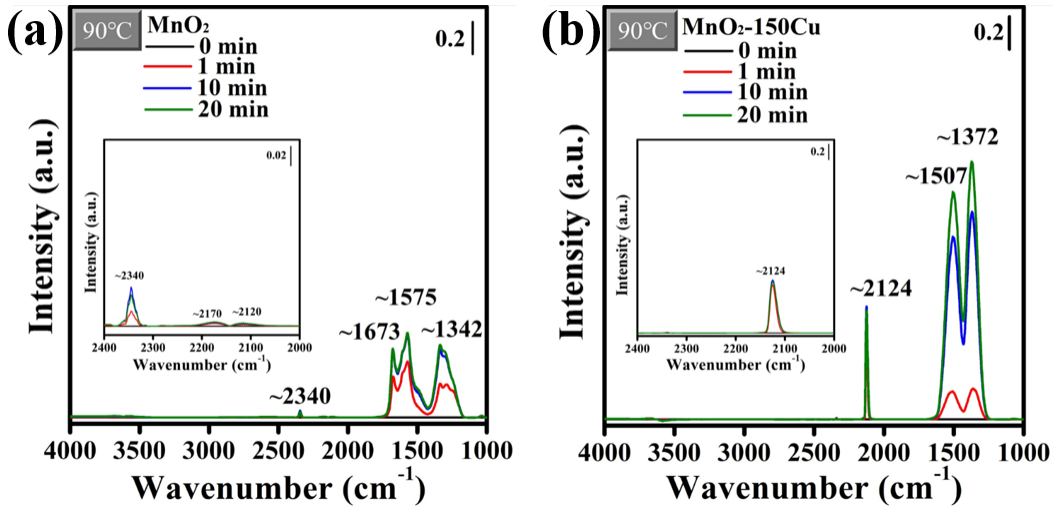

Fig. S8 In situ DRIFTS of (a) MnO_2 and (b) MnO_2-150Cu under dry 2% CO/O_2 at 90℃.

Table S1 Temperature of the first peak in H_2-TPR profiles of Cu-Mn oxide catalysts.

Catalyst name	Temperature of first peak (℃)	References
CuO-MnO_x-modified pinecone biochar	246	Yi et al. (2018)
Cu doped MnO_2	226	Zeng et al. (2020)
Metal-doped MnO_2 nanospheres	226	Peng et al. (2022)
Cu doped MnO_2	205	Zhang et al. (2021)
Cu-modified MnO_2	275	Shi et al. (2018)
Cu doped birnessite MnO_2	216	Yusuf et al. (2020)
MnO_2−CuO	202	Kim et al. (2017)
Cu–Mn composite catalyst	239	Dong et al. (2013)
Mn_2O_3@MnO_2-Cu	234	Yang et al. (2021)
Cu–MnO_2	255	Liu et al. (2018)
CuO/MnO_2	243	Qian et al. (2013)
Cu doped MnO_2	~350	Dong et al. (2020)
Copper − manganese Oxide	281	Liu et al. (2017)
CuO/α-MnO_2	262	May et al. (2020)
MnO_2-40Cu	199	this study
MnO_2-150Cu	199	this study

Table S2 Performance of various Cu-Mn oxides for CO oxidation under dry conditions.

Catalyst name	Space velocity (L/g·h)	CO concentration	Temperature at which CO conversion reached 100% (℃)	References
$CuMnO_x$	20	1%	70	Shi et al. (2015)
$CuMnO_x$	20	1%	140	Cai et al. (2014)
$Mn_{0.90}Cu_{0.10}O_2$	5.6	5%	140	Kunkalekar and Salker (2012)
$CuMnO_x$	36	2.5%	80	Dey et al. (2018)
$Cu_{1.5}Mn_{1.5}O_4$	600	4%	180	PalDey et al. (2005)
Cu/Mn = 1/2	150	1%	145	Hasegawa et al. (2009a)
Cu/Mn = 1/2	60	1%	125	Hasegawa et al. (2009b)
$CuMnO_x$	35	1%	30	Njagi et al. (2010)
Mn-Cu (0.1)	18	1%	100	Choi et al. (2016)
$CuMnO_{x\text{-}10}$	35	1%	25, 90 (> 12 h)	Njagi et al. (2011)
$Cu_{0.1}MnO_x$	36	1%	100	Gao et al. (2016)
Cu_1/MnO_2	15	1%	120	Hu et al. (2019)
$Cu_{0.075}Mn$	30	1.6%	65	Liu et al. (2017)
Cu-Mn oxide	120	0.5%	147	Einaga and Kiya (2016)
CuO/MnO_2	24	1%	110	Qian et al. (2013)
$7\%CuO/MnO_x$	10	1%	155	Peng et al. (2011)
$7Cu/MnO_2$	18	1%	115	Zhang et al. (2017)
$CuO/\alpha\text{-}MnO_2$	60	4%	> 100	Sadeghinia et al. (2013)
$CuO\text{-}MnO_2$	300	0.5%	160	Guo et al. (2017)
$CuO–MnO_2$	1.9	0.4%	98.1	Lin et al. (2017)
$Cu_{1.5}Mn_{1.5}O_4$	60	0.67%	110	Biemelt et al. (2016)
$CuO/\alpha\text{-}MnO_2$	80	1%	60	May et al. (2020)
CuO/MnO_x	60	1.9%	200	Gong et al. (2013)
Cu_1/MnO_2	15	1%	90	Hu et al. (2020)
MnO_2-150Cu	35	1%	20, 80 (15.5 h)	this study
MnO_2-150Cu	150	0.025 %	−10, 30 (4 h)	this study

Table S3 Activity of different Cu-Mn oxides for CO oxidation under humid conditions.

Catalyst	WHSV (L/g·h)	Concentration			CO conversion	References
		CO	O_2	H_2O		
SnO_2-Hopacalite	18	1%	21%	3%	70℃, 92% (5 h)	Liu et al. (2016)
Cu-α-MnO_2	36	1%	20%	2%	120℃, 90% (50 h)	Gao et al. (2016)
Layered Cu-Mn	40	0.1%	21%	1.6%	76℃, 90%	Wang et al. (2019)
CuO-α-MnO_2	80.4	1%	20%	3%	105℃, 100%; 90℃, ~60% (72 h)	May et al. (2020)
Sn-α-MnO_2	18	0.25%	10%	3.1%	179℃, 90%	Li et al. (2022)
F-Co_3O_4@CNT	35	1%	2%	3%	150℃, 100%	Kuo et al. (2014)
Meso- Co_3O_4	12	1%	1%	3%	80℃, 100%	Song et al. (2014)
La-doped Co_3O_4	120	0.4%	10%	3%	155℃, 90%	Bae et al. (2019)
Sn-doped Co_3O_4	15	1%	20%	0.5%	80℃, 70%	Feng et al. (2020)
0.2La-Pt-CoO/Al_2O_3	36	1%	1%	1630 ppm	−15℃, 100%	Xu et al. (2023)

References

Bae J, Shin D, Jeong H, Kim B S, Han J W, Lee H (2019). Highly water-resistant La-doped Co3O4 catalyst for CO oxidation. ACS Catalysis, 9(11): 10093–10100

Biemelt T, Wegner K, Teichert J, Lohe M R, Martin J, Grothe J, Kaskel S (2016). Hopcalite nanoparticle catalysts with high water vapour stability for catalytic oxidation of carbon monoxide. Applied Catalysis B: Environmental, 184: 208–215

Cai L, Hu Z, Branton P, Li W (2014). The effect of doping transition metal oxides on copper manganese oxides for the catalytic oxidation of CO. Chinese Journal of Catalysis, 35(2): 159–167

Choi K H, Lee D H, Kim H S, Yoon Y C, Park C S, Kim Y H (2016). Reaction characteristics of precious-metal-free ternary Mn–Cu–M (M = Ce, Co, Cr, and Fe) oxide catalysts for low-temperature CO oxidation. Industrial & Engineering Chemistry Research, 55(16): 4443–4450

Dey S, Dhal G C, Mohan D, Prasad R (2018). The choice of precursors in the synthesizing of CuMnOx catalysts for maximizing CO oxidation. International Journal of Industrial Chemistry, 9(3): 199–214

Dong C, Qu Z, Jiang X, Ren Y (2020). Tuning oxygen vacancy concentration of MnO2 through metal doping for improved toluene oxidation. Journal of Hazardous Materials, 391: 122181

Dong G, Li Y, Wang Y, Zhang J, Duan R (2013). DeNOx performance of Cu–Mn composite catalysts prepared by the slurry coating method. Reaction Kinetics, Mechanisms and Catalysis, 111(1): 235–245

Einaga H, Kiya A (2016). Effect of aging on the CO oxidation properties of copper manganese oxides prepared by hydrolysis–coprecipitation using tetramethyl ammonium hydroxide. Reaction Kinetics, Mechanisms and Catalysis, 117(2): 521–536

Feng B, Shi M, Liu J, Han X, Lan Z, Gu H, Wang X, Sun H, Zhang Q, Li H, Wang Y, Li H (2020). An efficient defect engineering strategy to enhance catalytic performances of Co3O4 nanorods for CO oxidation. Journal of Hazardous Materials, 394: 122540

Gao J, Jia C, Zhang L, Wang H, Yang Y, Hung S F, Hsu Y Y, Liu B (2016). Tuning chemical bonding of MnO2 through transition-metal doping for enhanced CO oxidation. Journal of Catalysis, 341: 82–90

Gong L, Huang Z, Luo L, Zhang N (2013). Promoting effect of MnOx on the performance of CuO/CeO2 catalysts for preferential oxidation of CO in H2-rich gases. Reaction Kinetics, Mechanisms and Catalysis, 111(2): 489–504

Guo Y, Zhao C, Lin J, Li C, Lu S (2017). Facile synthesis of supported copper manganese oxides catalysts for low temperature CO oxidation in confined spaces. Catalysis Communications, 99: 1–5

Hasegawa Y I, Maki R U, Sano M, Miyake T (2009a). Preferential oxidation of CO on copper-containing manganese oxides. Applied Catalysis A, General, 371(1–2): 67–72

Hasegawa Y, Fukumoto K, Ishima T, Yamamoto H, Sano M, Miyake T (2009b). Preparation of copper-containing mesoporous manganese oxides and their catalytic performance for CO oxidation. Applied Catalysis B: Environmental, 89(3–4): 420–424

Hu X, Chen J, Li S, Chen Y, Qu W, Ma Z, Tang X (2019). The promotional effect of copper in catalytic oxidation by Cu-doped α-MnO2 nanorods. Journal of Physical Chemistry C, 124(1): 701–708

Hu X, Li S, Chen Y, Qu W, Chen J, Ma Z, Tang X (2020). Single-ion copper doping greatly enhances catalytic activity of manganese oxides via electronic interactions. Chemical Communications (Cambridge), 56(6): 904–907

Kim J, Min Y H, Lee N, Cho E, Kim K Y, Jeong G, Moon S K, Joo M, Kim D B, Kim J, Kim S Y, Kim Y, Oh J, Sato S (2017). In situ spectroscopic and computational studies on a MnO2-CuO catalyst for use in volatile organic compound decomposition. ACS Omega, 2(10): 7424–7432

Kunkalekar R K, Salker A V (2012). Low temperature CO oxidation over nano-sized Cu–Pd doped MnO2 catalysts. Reaction Kinetics, Mechanisms and Catalysis, 108: 173–182

Kuo C H, Li W, Song W, Luo Z, Poyraz A S, Guo Y, Ma A W, Suib S L, He J (2014). Facile synthesis of Co3O4@CNT with high catalytic activity for CO oxidation under moisture-rich conditions. ACS Applied Materials & Interfaces, 6(14): 11311–11317

Li G, Zhao Z, Zhao T, Li W, Wei Z, Duan X, Zhang Z, Cheng J, Hao Z (2022). Tin-doped manganese octahedral molecular sieve catalysts with efficient water resistance for CO oxidation. Catalysis Today, 405–406: 337–347

Lin J, Guo Y, Chen X, Li C, Lu S, Liew K M (2017). CO oxidation over nanostructured ceria supported bimetallic Cu–Mn oxides catalysts: Effect of Cu/Mn ratio and calcination temperature. Catalysis Letters, 148(1): 181–193

Liu T, Yao Y, Wei L, Shi Z, Han L, Yuan H, Li B, Dong L, Wang F, Sun C (2017). Preparation and evaluation of copper–manganese oxide as a high-efficiency catalyst for CO oxidation and NO reduction by CO. Journal of Physical Chemistry C, 121(23): 12757–12770

Liu Y, Guo Y, Peng H, Xu X, Wu Y, Peng C, Zhang N, Wang X (2016). Modifying hopcalite catalyst by SnO2 addition: An effective way to improve its moisture tolerance and activity for low temperature CO oxidation. Applied Catalysis A, General, 525: 204–214

Liu Y, Zong W, Zhou H, Wang D, Cao R, Zhan J, Liu L, Jang B W L (2018). Tuning the interlayer cations of birnessite-type MnO2 to enhance its oxidation ability for gaseous benzene with water resistance. Catalysis Science & Technology, 8(20): 5344–5358

May Y A, Wei S, Yu W Z, Wang W W, Jia C J (2020). Highly efficient CuO/α-MnO2 catalyst for low-temperature CO oxidation. Langmuir, 36(38): 11196–11206

Njagi E C, Chen C H, Genuino H, Galindo H, Huang H, Suib S L (2010). Total oxidation of CO at ambient temperature using copper manganese oxide catalysts prepared by a redox method. Applied Catalysis B: Environmental, 99(1–2): 103–110

Njagi E C, Genuino H C, King'ondu C K, Chen C H, Horvath D, Suib S L (2011). Preferential oxidation of CO in H2-rich feeds over mesoporous copper manganese oxides synthesized by a redox method. International Journal of Hydrogen Energy, 36(11): 6768–6779

PalDey S, Gedevanishvili S, Zhang W, Rasouli F (2005). Evaluation of a spinel based pigment system as a CO oxidation catalyst. Applied Catalysis B: Environmental, 56(3): 241–250

Peng C T, Lia H K, Liaw B J, Chen Y Z (2011). Removal of CO in excess hydrogen over CuO/Ce1−xMnxO2 catalysts. Chemical Engineering Journal, 172(1): 452–458

Peng K, Hou Y, Zhang Y, Liu X, Li Y, Li B, Zeng Z, Huang Z (2022). Engineering oxygen vacancies in metal-doped MnO2 nanospheres for boosting the low-temperature toluene oxidation. Fuel, 314: 123123

Qian K, Qian Z, Hua Q, Jiang Z, Huang W (2013). Structure–activity relationship of CuO/MnO2 catalysts in CO oxidation. Applied Surface Science, 273: 357–363

Sadeghinia M, Rezaei M, Amini E (2013). Preparation of α-MnO2 nanowires and its application in low temperature CO oxidation. Korean Journal of Chemical Engineering, 30(11): 2012–2016

Shi C, Chang H, Wang C, Zhang T, Peng Y, Li M, Wang Y, Li J (2018). Improved activity and H2O resistance of Cu-modified MnO2 catalysts for NO oxidation. Industrial & Engineering Chemistry Research, 57(3): 920–926

Shi L, Hu Z H, Deng G M, Li W C (2015). Carbon monoxide oxidation on copper manganese oxides prepared by selective etching with ammonia. Chinese Journal of Catalysis, 36(11): 1920–1927

Song W, Poyraz A S, Meng Y, Ren Z, Chen S Y, Suib S L (2014). Mesoporous Co3O4 with controlled porosity: Inverse micelle synthesis and high-performance catalytic CO oxidation at −60℃. Chemistry of Materials, 26(15): 4629–4639

Wang Y, Yang D, Li S, Zhang L, Zheng G, Guo L (2019). Layered copper manganese oxide for the efficient catalytic CO and VOCs oxidation. Chemical Engineering Journal, 357: 258–268

Xu L, Pan Y, Li H, Xu R, Sun Z (2023). Highly active and water-resistant Lanthanum-doped platinum-cobalt oxide catalysts for CO oxidation. Applied Catalysis B: Environmental, 331: 122678

Yang W, Wang Y, Yang W, Liu H, Li Z, Peng Y, Li J (2021). Surface in situ doping modification over Mn2O3 for toluene and propene catalytic oxidation: The effect of isolated Cuδ+ insertion into the mezzanine of surface MnO2 cladding. ACS Applied Materials & Interfaces, 13(2): 2753–2764

Yi Y, Li C, Zhao L, Du X, Gao L, Chen J, Zhai Y, Zeng G (2018). The synthetic evaluation of CuO-MnOx-modified pinecone biochar for simultaneous removal formaldehyde and elemental mercury from simulated flue gas. Environmental Science and Pollution Research International, 25(5): 4761–4775

Yusuf A, Sun Y, Ren Y, Snape C, Wang C, Jia H, He J (2020). Opposite effects of Co and Cu dopants on the catalytic activities of birnessite MnO2 catalyst for low-temperature formaldehyde oxidation. Journal of Physical Chemistry C, 124(48): 26320–26331

Zeng X, Li B, Liu R, Li X, Zhu T (2020). Investigation of promotion effect of Cu doped MnO2 catalysts on ketone-type VOCs degradation in a one-stage plasma-catalysis system. Chemical Engineering Journal, 384: 123362

Zhang L, Wang S, Ni C, Wang M, Wang S (2021). Ozone elimination over oxygen-deficient MnOx based catalysts: Effect of different transition metal dopants. Chemical Engineering Science, 229: 116011

Zhang X, Li H, Yang Y, Zhang T, Wen X, Liu N, Wang D (2017). Facile synthesis of new efficient Cu/MnO2 catalysts from used battery for CO oxidation. Journal of Environmental Chemical Engineering, 5(5): 5179–5186